Material Properties of the Postsynaptic Density Condensate Set AMPA-Receptor Retention Time: A Quantitative Phase-Separation and Escape-Kinetics Model of LTP Maintenance

Brent S. Hartshorn

July 29, 2026

Abstract

A central puzzle in synaptic plasticity is how long-term potentiation (LTP) is *maintained* for hours to days despite continuous turnover of synaptic proteins. Recent experiments reframe the problem in physical terms: the postsynaptic density (PSD) is a biomolecular condensate whose *material state*—its network connectivity and viscoelasticity—is causally coupled to AMPA-receptor (AMPAR) mobility and to plasticity. In particular, weakening scaffold percolation softens the PSD condensate, increases AMPAR mobility, and impairs plasticity, while CaMKII maintenance of LTP appears to be a structural (binding) rather than a downstream-enzymatic effect. These results are qualitative. Here we supply the missing quantitative framework. We model the PSD as a multivalent condensate using a Flory–Huggins free energy augmented by a percolation (gelation) order parameter, and we treat AMPAR retention as Kramers escape from the free-energy well created by the condensate. The model yields three results. (i) The receptor residence time depends *exponentially* on scaffold connectivity, so that retention collapses by orders of magnitude when the network is driven below its percolation threshold—a sharp "depotentiation cliff" rather than a graded loss. (ii) Treating an AMPAR nanodomain as a capillary cluster gives a critical size of tens of nanometres from independently measured condensate surface tension and binding-site concentration, an order-of-magnitude match to the ∼70–80 nm nanodomains seen by super-resolution microscopy. (iii) The framework reproduces, without invoking any downstream phosphorylation, why binding-competent but enzymatically dead CaMKII can sustain potentiation: the memory variable is the material state of the condensate, not the phosphorylation state of an effector. We give a parameter table with sources and uncertainties, and three quantitative, falsifiable predictions that distinguish this model from a purely biochemical account. We make no claims beyond synaptic biophysics; nothing here concerns quantum coherence, consciousness, or non-local correlations.

1 Introduction

1.1 The maintenance problem

Long-term potentiation is the leading cellular model for learning and memory, and CaMKII is its central molecular actor. A long-standing difficulty is that the molecules implicated in LTP—CaMKII, PSD-95, AMPARs, TARPs—exchange with the cytosol on timescales (seconds to minutes) far shorter than the memory they support (hours to a lifetime). Any mechanistic account of *maintenance* must therefore locate the stored variable in something more persistent than the occupancy of any single molecule.

1.2 The postsynaptic density is a condensate

A decade of reconstitution work has established that the core PSD scaffolds (PSD-95, GKAP/SAPAP, Shank, Homer, together with SynGAP and receptor tails) undergo liquid–liquid phase separation (LLPS) to form a dense, selective, membrane-apposed compartment that concentrates AMPAR/TARP complexes [1, 2]. Phosphorylation of scaffold residues tunes this phase behaviour [3], and additional disordered components (e.g. FAM81A) promote condensation [4]. The PSD is thus not a rigid lattice but a tunable soft material.

1.3 Material state is causally coupled to plasticity

Two recent results sharpen this into a mechanistic target. First, Chen et al. [5] showed that autophosphorylation of CaMKII at Thr286 *together with* long-lasting binding to GluN2B is the minimal requirement for LTP maintenance, and that a kinase-dead but conformationally open CaMKII can still potentiate—i.e. the maintenance action is plausibly *structural* rather than enzymatic. (We note this remains debated; an alternative view assigns pThr286 mainly to induction-phase signalling [6].) Second, and most directly, condensate *material properties* have been tied to receptor dynamics: weakening the percolation of the scaffold network (by converting a Shank3 oligomerization domain to a monomer) softens the PSD condensate, increases AMPAR mobility, and impairs synaptic transmission and plasticity [7]. Photoactivation studies likewise couple CaMKII recruitment, condensate remodelling, and AMPAR accumulation [8].

1.4 What is missing, and our contribution

These findings are qualitative: stiffer/more-percolated condensate ⇒ less receptor mobility ⇒ stronger, more stable synapse. What is missing is a quantitative framework that (a) specifies how scaffold binding and valency move the condensate across its phase and percolation boundaries, (b) converts the condensate material state into a measurable receptor *retention time*, and (c) yields parameter-specific, falsifiable predictions. We supply that framework using standard soft-matter physics—Flory–Huggins phase separation, Flory–Stockmayer gelation, sticky-network rheology, and Kramers escape kinetics—applied to the synaptic problem. The novelty is not new physics but the quantitative mapping and the predictions it generates. **Scope.** This is a biophysical model of receptor retention. It makes no claim about consciousness, agency, quantum coherence, or nonlocal correlations, and it does not depend on any such notion.

2 Phase behaviour of the PSD condensate

2.1 Flory–Huggins baseline

Let ϕ be the volume fraction of the multivalent scaffold network and N an effective degree of polymerization (a proxy for scaffold valency/connectivity). The Flory–Huggins free-energy density (in units of $k_{\mathrm{B}}T$ per lattice site) is

$$f(\phi) = \frac{\phi}{N}\ln\phi + (1-\phi)\ln(1-\phi) + \chi\,\phi(1-\phi), \tag{1}$$

where χ is the effective interaction parameter aggregating scaffold–scaffold and CaMKII–GluN2B–scaffold attractions. Phase coexistence (the binodal) follows from the common-tangent construction $f'(\phi_a) = f'(\phi_b)$ and $f(\phi_a) - \phi_a f'(\phi_a) = f(\phi_b) - \phi_b f'(\phi_b)$, giving the dilute-branch saturation concentration $c_{\mathrm{sat}} \equiv \phi_a$ and the dense-phase fraction ϕ_b.

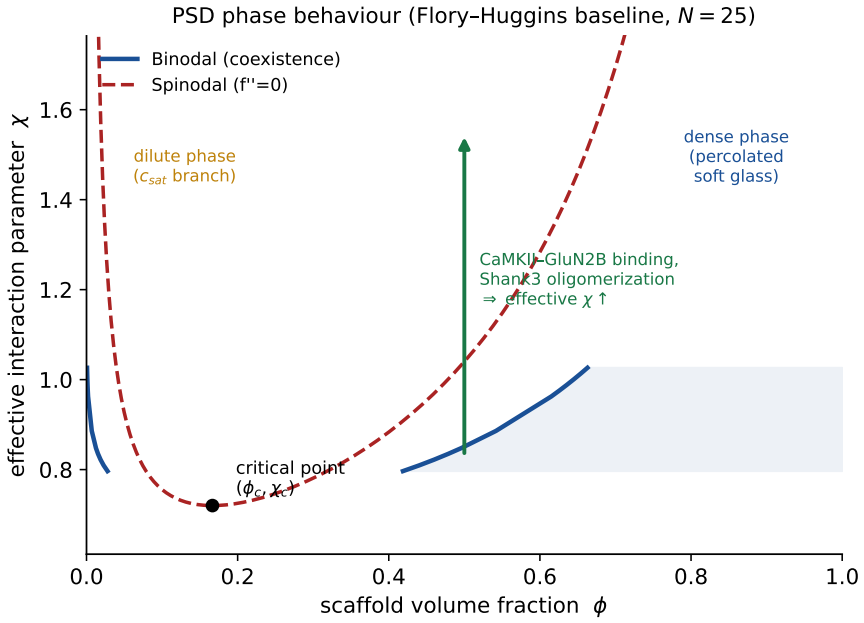

Figure 1: **PSD phase behaviour.** Flory–Huggins binodal (blue) and spinodal (red dashed) for effective valency $N = 25$, with critical point $(\phi_c, \chi_c) = (0.167, 0.72)$. Activity-dependent CaMKII–GluN2B binding and Shank3 oligomerization raise the effective interaction parameter χ (green arrow), carrying the synapse into the dense, percolated regime (shaded). The dilute branch defines the saturation concentration c_{sat}.

The limit of metastability (the spinodal, $f'' = 0$) and the critical point have closed forms:

$$\chi_{\mathrm{sp}}(\phi) = \frac{1}{2}\left(\frac{1}{N\phi} + \frac{1}{1-\phi}\right), \qquad \phi_c = \frac{1}{1+\sqrt{N}}, \qquad \chi_c = \frac{1}{2}\left(1 + \frac{1}{\sqrt{N}}\right)^2. \tag{2}$$

For $N = 25$ (a representative effective valency) these give $\phi_c = 0.167$ and $\chi_c = 0.72$. Figure 1 shows the computed binodal and spinodal. The biological control variables—local CaMKII concentration, the fraction of CaMKII bound to GluN2B, and Shank3 oligomerization state—enter through the effective χ and N: activity-driven binding *raises* the effective attraction, driving the synapse from the one-phase (dilute) region across the binodal into robust two-phase coexistence.

2.2 Percolation: from droplet to soft glass

Phase separation alone gives a liquid droplet; the measured PSD condensate is a *soft glass* whose rigidity tracks network connectivity [7]. This is the regime of phase separation coupled to percolation (PSCP) [9]. For a network of scaffolds with functionality f (number of binding sites per node) and bond-occupancy probability p (fraction of sites engaged), the Flory–Stockmayer gel point is

$$p_c = \frac{1}{f-1}. \tag{3}$$

For tetravalent scaffolds ($f = 4$), $p_c = 1/3$. Above p_c a system-spanning network exists, with order parameter (gel fraction)

$$P_\infty(p) = \begin{cases} \left(\dfrac{p - p_c}{1 - p_c}\right)^\beta, & p > p_c, \\ 0, & p \le p_c, \end{cases} \tag{4}$$

with $\beta \approx 0.41$ for three-dimensional percolation. The bond occupancy p is set by binding affinities and local concentrations and is therefore the quantity that CaMKII–GluN2B binding and scaffold oligomerization control. P_∞ is the material-state variable that enters the retention model below.

3 Rheology of the condensate

Treating the percolated scaffold as a transient (sticky) network, the linear viscoelastic response is approximately Maxwellian,

$$G(t) = G_0\, e^{-t/\tau_{\mathrm{relax}}}, \qquad \eta \simeq G_0\, \tau_{\mathrm{relax}}, \tag{5}$$

where G_0 is the network plateau modulus and τ_{relax} the terminal relaxation time. For a sticky network the relaxation time is set by the bond lifetime $\tau_b = \tau_0 e^{E_b/k_{\mathrm{B}}T}$ and diverges as connectivity approaches its limit; near the gel point a convenient scaling is $\tau_{\mathrm{relax}} \sim \tau_b\, [P_\infty(p)]^{-z}$ with a dynamic exponent $z > 0$. The qualitative consequence matches experiment: increasing connectivity stiffens the condensate ($G_0 \uparrow$, $\eta \uparrow$) and slows internal rearrangement, while monomerization softens it [7]. The plateau modulus and viscosity are the experimentally accessible handles (active microrheology, FRAP) that the next section ties to receptor retention.

4 AMPAR retention as Kramers escape

4.1 Partitioning and the retention time

AMPAR/TARP complexes are enriched in the PSD with a partition coefficient

$$K = \frac{c_{\mathrm{dense}}}{c_{\mathrm{dilute}}} = \exp\!\left(-\frac{\Delta\mu}{k_{\mathrm{B}}T}\right), \tag{6}$$

where $\Delta\mu < 0$ is the transfer free energy of a receptor complex from the dilute phase into the condensate. Receptor capture and loss is a barrier-crossing process: a receptor leaves the synapse only by escaping the free-energy well created jointly by direct scaffold binding (PSD-95/TARP) and by partitioning into the dense phase. By Kramers' theory the mean residence time is

$$\boxed{\tau_{\mathrm{res}} = \tau_0\, \exp\!\left(\frac{\Delta G_{\mathrm{eff}}}{k_{\mathrm{B}}T}\right)} \qquad \Delta G_{\mathrm{eff}} = \Delta G_{\mathrm{bind}} + \Delta G_{\mathrm{cond}}, \tag{7}$$

where τ_0 is a microscopic attempt time (∼ms, set by local membrane diffusion over the trap width) and ΔG_{cond} is the contribution of the condensate to the trapping barrier.

4.2 Coupling retention to material state

The condensate contribution scales with how completely the network is percolated—a fully connected, rigid scaffold presents the deepest well, a sub-percolation soup presents none. We therefore write

$$\Delta G_{\mathrm{cond}} = \Delta G_{\max}\, P_\infty(p), \tag{8}$$

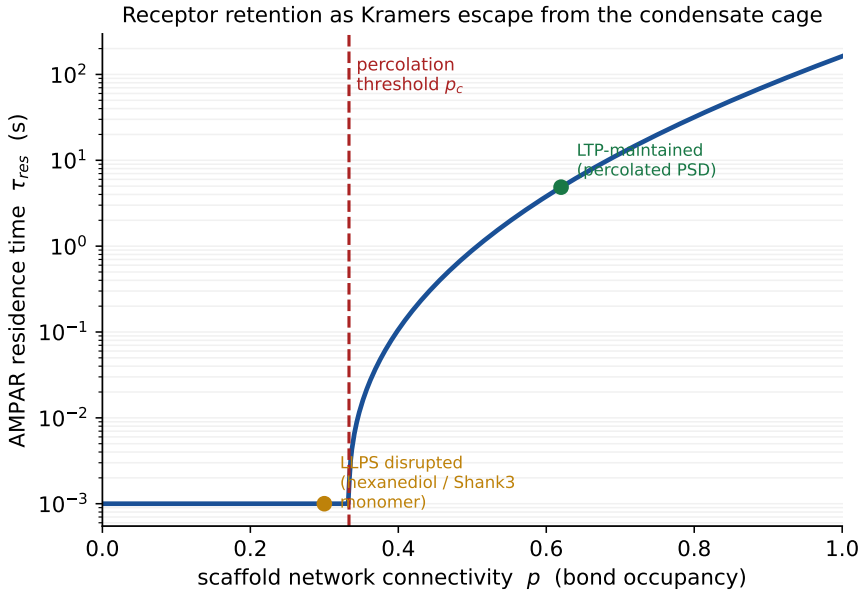

Figure 2: **Receptor retention as Kramers escape.** Mean AMPAR residence time τ_{res} (log scale) versus scaffold connectivity p from Eq. (9) ($\Delta G_{\max} = 12\,k_{\mathrm{B}}T$, $\tau_0 = 1$ ms, $\beta = 0.41$, $p_c = 1/3$). Above the percolation threshold (red dashed) retention rises steeply; below it, retention collapses to the bare attempt time. A perturbation that lowers effective connectivity (hexanediol, Shank3 monomerization) produces an order-of-magnitude loss of retention—the depotentiation cliff—even with binding partners present.

with $\Delta G_{\max}$ the maximal partition/caging free energy at full percolation. Combining (4), (7), (8):

$$\tau_{\mathrm{res}}(p) = \tau_0 \exp\left[\frac{\Delta G_{\mathrm{bind}}}{k_{\mathrm{B}}T} + \frac{\Delta G_{\max}}{k_{\mathrm{B}}T}\left(\frac{p - p_c}{1 - p_c}\right)^{\beta}\right], \quad p > p_c. \tag{9}$$

Because ΔG_{cond} enters the exponent, retention is *exponentially* sensitive to connectivity. Figure 2 plots $\tau_{\mathrm{res}}(p)$ for $\Delta G_{\max} = 12\,k_{\mathrm{B}}T$ and $\tau_0 = 1$ ms: a percolated synapse holds receptors for seconds-to-minutes, but driving p below p_c (by LLPS disruption or scaffold monomerization) collapses retention to the bare τ_0—a fall of several orders of magnitude across a narrow window. This is the quantitative form of the "depotentiation cliff": maintenance is not lost gradually but catastrophically once the network de-percolates.

4.3 From retention time to synaptic weight

If receptors are supplied to the synapse at rate J_{in} and lost with rate $1/\tau_{\mathrm{res}}$, the steady-state bound number is $n = J_{\mathrm{in}}\,\tau_{\mathrm{res}}$, and the synaptic weight (proportional to synaptic AMPAR number) inherits the exponential dependence on material state. Maintenance of LTP then requires only that the condensate remain percolated; it does *not* require ongoing phosphorylation of any downstream effector. This is precisely the regime of Chen et al. [5]: binding-competent CaMKII keeps the network above p_c (structural role), and the stored variable is P_∞, a property of the material, not the phosphorylation state of AMPARs or TARPs.

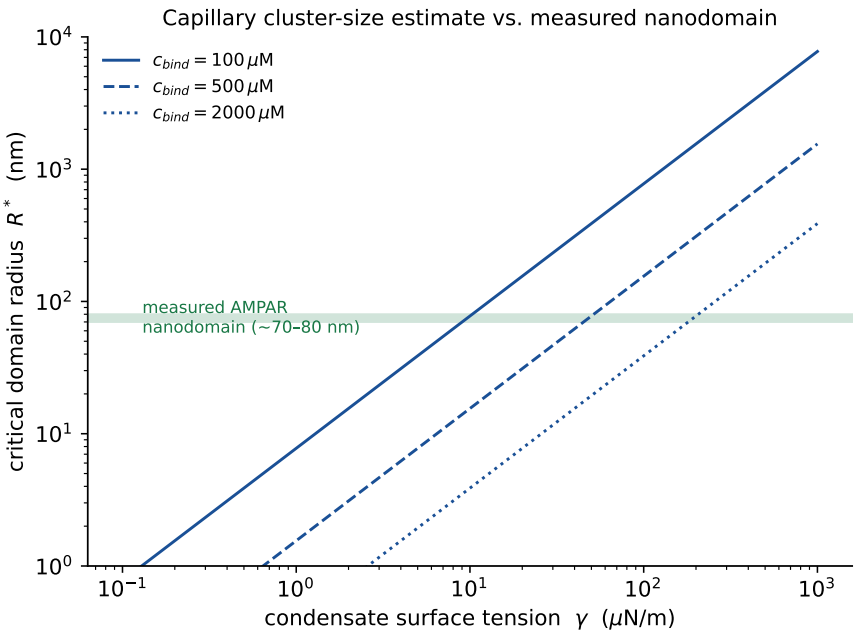

Figure 3: **Capillary cluster-size estimate.** Critical domain radius R^* versus condensate surface tension γ from Eq. (10), for three binding-site concentrations. The green band marks the measured AMPAR nanodomain size (∼70–80 nm). The estimate lands within an order of magnitude across physiological parameter ranges, without tuning.

5 Nanodomain size from capillarity

Super-resolution microscopy shows AMPARs organised into nanodomains of ∼70–80 nm containing ∼20 receptors, aligned with presynaptic release sites [10, 11]. We ask whether condensate physics predicts this scale. Treating a nanodomain as a condensed cluster, the competition between surface (interfacial) energy and bulk free-energy gain gives the classical critical radius

$$R^* = \frac{2\gamma}{\Delta f}, \qquad \Delta f \simeq k_{\mathrm{B}} T\, c_{\mathrm{bind}}, \tag{10}$$

with γ the condensate surface tension and c_{bind} the number density of binding sites driving supersaturation. For protein condensates $\gamma \sim 1$–$100\,\mu$N/m and synaptic binding-site concentrations $c_{\mathrm{bind}} \sim 10^2$–$10^3\,\mu$M, Eq. (10) gives $R^* \sim 10$–10^2 nm (Fig. 3); at $\gamma = 10\,\mu$N/m, $c_{\mathrm{bind}} = 500\,\mu$M one finds $R^* \approx 16$ nm. The measured 70–80 nm band is reached at the lower-supersaturation / higher-tension corner. Because the AMPAR nanodomain is membrane-embedded, the physically cleaner statement uses a two-dimensional line tension λ, $R^*_{\mathrm{2D}} = \lambda/\Delta f_{\mathrm{2D}}$, which for $\lambda \sim 1$ pN and areal binding-site densities $\sim 10^{15}$–$10^{16}\,\mathrm{m}^{-2}$ gives the same tens-of-nanometres scale. We present this as an order-of-magnitude consistency, not a precise prediction: the relevant interfacial parameters for the PSD have not been directly measured (see §8).

6 Parameters

Table 1 lists the model parameters, representative values, and sources, flagging which are well-constrained and which are estimates. The predictions in §7 are stated as *scalings* precisely because

Symbol	Meaning	Value (310 K)	Source / status
k_BT	thermal energy	4.28×10^{-21} J	exact
N	effective scaffold valency	∼10–50	estimate (PSCP proxy)
ϕ_c, χ_c	critical point	0.167, 0.72 (N=25)	from Eq. (2)
f	scaffold functionality	3–6	PSD-95/Shank/SynGAP multivalency
p_c	percolation threshold	$1/(f-1)$	Flory–Stockmayer
β	percolation exponent	0.41	3D universality
ΔG_{max}	max. caging free energy	∼8–15 k_BT	estimate (FRAP/partition)
τ_0	attempt time	∼1–10 ms	membrane diffusion over trap
τ_{res}	receptor residence time	s–min	FRAP, sptPALM [10]
γ	condensate surface tension	1–100 μN/m	protein condensates; PSD not yet measured
η	condensate viscosity	0.1–10^3 Pa s	soft-glass range [7]
c_{bind}	binding-site density	10^2–10^3 μM	PSD scaffold estimates
R^*	nanodomain radius	∼35–40 nm	[10, 11]

Table 1: Model parameters with sources and uncertainty status.

several interfacial parameters remain unmeasured.

7 Three falsifiable predictions

Each prediction is quantitative and distinguishes the material-state model from a purely biochemical (phosphorylation-occupancy) account. We deliberately do *not* rest the central test on 1,6-hexanediol alone—it has well-known off-target effects on kinases and membranes—but pair it with genetic valency control and optogenetic condensate tuning.

Prediction 1 (depotentiation cliff).

Synaptic AMPAR retention is a *threshold*, not graded, function of scaffold connectivity. As connectivity is lowered (titrated Shank3 monomerization, or graded optogenetic de-clustering), τ_{res} should fall steeply once the network crosses p_c, following Eq. (9): a near-flat region above threshold and an order-of-magnitude collapse below it. *Readout:* FRAP/sptPALM residence times vs. a tunable valency series. *Falsified if* retention declines linearly with connectivity with no threshold.

Prediction 2 (maintenance is structural, not enzymatic).

Disrupting the condensate *after* LTP induction reverses potentiation even when CaMKII autophosphorylation and GluN2B binding are intact. *Readout:* field EPSPs after post-induction LLPS disruption, with three arms—(i) hexanediol; (ii) acute optogenetic condensate dissolution (preferred, specific); (iii) Shank3 SAM-monomer knock-in. All three should depotentiate without requiring loss of pThr286. *Falsified if* potentiation persists when the condensate is dissolved but CaMKII remains bound.

Prediction 3 (rheology–retention scaling).

Receptor residence time tracks a measurable material property. Across conditions that vary connectivity, $\ln \tau_{\mathrm{res}}$ should be linear in the condensate plateau modulus G_0 (equivalently in P_∞), with a slope set by $\Delta G_{\max}/k_{\mathrm{B}}T$. *Readout:* active microrheology of reconstituted PSD condensates (G_0, η) combined with single-molecule receptor retention in the same preparation. *Falsified if* retention is uncorrelated with condensate stiffness.

8 Limitations and scope

The model uses deliberately coarse, standard tools, and its limits should be stated plainly. (1) Flory–Huggins and classical nucleation are mean-field approximations; real PSD scaffolds are sequence-specific stickers-and-spacers polymers, and the membrane setting is two-dimensional. We use the mean-field forms as transparent baselines and flag where the membrane/2D refinement matters. (2) Several interfacial parameters (γ, λ, $\Delta G_{\max}$) have not been directly measured for the PSD; consequently our nanodomain result is an order-of-magnitude consistency and our retention predictions are stated as *scalings* rather than absolute numbers. (3) The causal direction (material state $\rightarrow$ receptor retention $\rightarrow$ plasticity) has qualitative experimental support [7, 5], but the specific exponential and threshold scalings derived here are, as yet, untested—which is the point of §7. (4) The model addresses receptor retention and LTP maintenance only. It is silent on induction-phase signalling, on metaplasticity, and on anything outside synaptic biophysics; in particular it neither requires nor supports any claim about quantum effects or consciousness.

9 Discussion

The picture that emerges is economical. Activity drives CaMKII to bind GluN2B and scaffolds to oligomerize; this raises the effective interaction parameter and the bond occupancy, carrying the PSD across its phase boundary and—crucially—above its percolation threshold (§2). The resulting percolated soft glass deepens the free-energy well that traps AMPARs, and because that well enters the escape rate exponentially, a modest, switch-like change in connectivity produces a large, persistent change in receptor retention and hence synaptic weight (§4). The stored memory variable is the connectivity/material state of the condensate, which is robust to single-molecule turnover in the same way a gel's rigidity is robust to the exchange of individual crosslinks. This directly rationalises why binding-competent but enzymatically inactive CaMKII suffices for maintenance [5], and why softening the network impairs plasticity [7].

The framework also organises several otherwise-disparate observations. Activity-dependent down-scaling of PSD size during sleep, driven by Homer1a [1], is naturally read as a controlled reduction of connectivity (lowering p toward p_c), predicted here to reduce retention sharply rather than gradually. Pathological loss of scaffold integrity—whether by mutation (autism-associated Shank3 truncations [7]) or by sequestration of components—appears as de-percolation, with the depotentiation cliff as its functional signature. We emphasise that these are connections to be tested by the quantitative scalings of §7, not claims of having explained the phenomena.

10 Conclusion

We have given a quantitative, falsifiable account of LTP maintenance as a material-state property of the PSD condensate, built entirely from standard soft-matter physics and anchored to recent experiments that tie condensate mechanics to receptor mobility and plasticity. The model's central, testable claim is that receptor retention depends exponentially on scaffold connectivity, producing a percolation-threshold "cliff" that a purely biochemical account does not predict. The accompanying predictions are accessible with existing methods—tunable-valency genetics, optogenetic condensate control, active microrheology, and single-molecule receptor tracking—and would either substantiate or refute the framework on quantitative grounds.

A Speculative Extension: Isotopic Control of Condensate Material State and Receptor Retention

Status of this appendix

The main text is built only from measured quantities and standard physics, and its predictions stay inside synaptic biophysics. This appendix is deliberately more speculative. We separate two layers explicitly: (i) a *thermodynamic* prediction (§A.2–§A.4) that follows from the main-text model and from *measured* solvent-isotope effects on phase separation, and is testable on its own; and (ii) a *conjectural* vibrational interpretation (§A.5) that connects to prior, more radical proposals [16, 17] and is *not* required by, and does not strengthen, the thermodynamic prediction. Nothing here invokes quantum coherence, non-locality, or agency; the falsifiable claim below is ordinary thermodynamics.

A.1 Measured premise

Solvent deuteration is not inert toward phase separation. Replacing even small fractions of H_2O with D_2O measurably increases the LLPS propensity of a disordered protein domain, an effect attributed to strengthening of the hydrophobic interactions that drive condensation [13]; deuteration systematically alters protein and membrane thermodynamics [14]; and condensates can act as physiological sensors of water potential [15]. Together these establish that the *isotopic and activity state of solvent water* is a genuine control parameter on condensate stability—and therefore, through the main-text model, on receptor retention.

A.2 Isotope substitution as a shift in the interaction parameter

Write the effective Flory–Huggins parameter with a linear isotope term,

$$\chi(T, x_D) \approx \chi_0(T) + \kappa\, x_D, \tag{11}$$

where x_D is the D_2O mole fraction. The coefficient $\kappa = \partial\chi/\partial x_D$ is *measurable*: along the experimental cloud-point curve χ is fixed at its binodal value, so $(\partial\chi/\partial T)\, dT^* + \kappa\, dx_D = 0$, giving

$$\kappa = -\left(\frac{\partial\chi}{\partial T}\right)\left(\frac{dT^*}{dx_D}\right)_{\text{cloud}}. \tag{12}$$

For a lower-critical-solution-temperature (hydrophobically driven) system, $\partial\chi/\partial T > 0$ and the cloud point falls with added D_2O ($dT^*/dx_D < 0$) [13], so $\kappa > 0$: D_2O deepens the effective

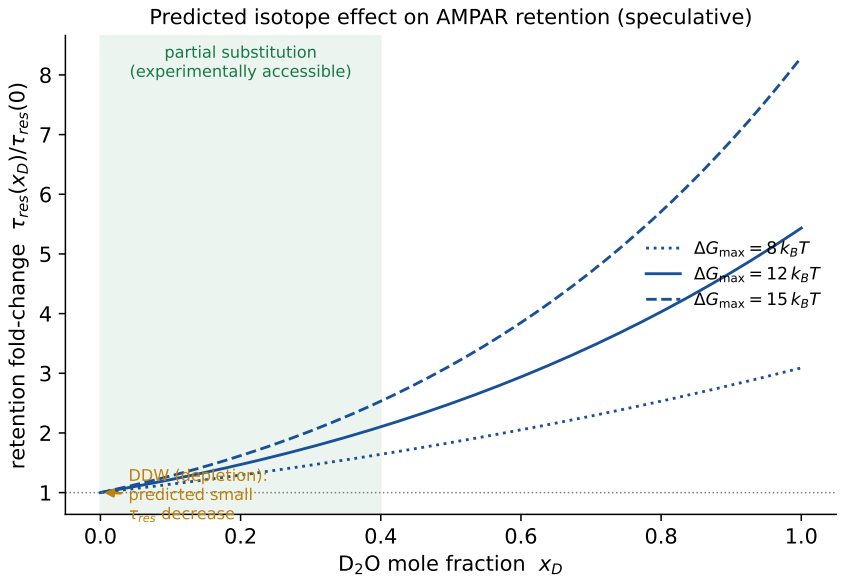

Figure 4: **Predicted isotope effect on receptor retention (speculative).** Fold-change in AMPAR residence time vs. D_2O mole fraction from Eq. (13), for three values of the caging free energy $\Delta G_{\max}$ ($p_0 = 0.5$, $g = 0.12$, $\beta = 0.41$, $p_c = 1/3$). The shaded band marks experimentally accessible partial substitution. Deuterium depletion (DDW) lies at the lower-left and is predicted to produce only a small *decrease* in retention, because natural D abundance ($x_D \approx 1.6 \times 10^{-4}$) is already tiny.

attraction, exactly as required for it to promote condensation. (The sign reverses for predominantly electrostatically driven condensates; the PSD prediction below therefore applies specifically to the hydrophobically driven component of scaffold interactions, and its sign is itself a test of which interactions dominate.)

A.3 Propagation to receptor retention

A shift in χ shifts the bond occupancy p that sets network percolation, $\delta p = (\partial p/\partial \chi)\,\kappa\, x_D \equiv g\, x_D$, where g is an effective connectivity gain per unit D_2O. Inserting into the retention law of Eq. (9) gives a parameter-free *form* for the fold-change in residence time,

$$\frac{\tau_{\rm res}(x_D)}{\tau_{\rm res}(0)} = \exp\left[\frac{\Delta G_{\max}}{k_{\rm B}T}\Big(P_\infty(p_0 + g\, x_D) - P_\infty(p_0)\Big)\right]. \tag{13}$$

Because retention depends exponentially on the percolation order parameter, even a modest isotope-induced connectivity gain produces a several-fold change in retention. For an illustrative operating point ($p_0 = 0.5$, $g = 0.12$, $\Delta G_{\max} = 12\,k_{\rm B}T$), Eq. (13) gives $\tau_{\rm res}(0.5)/\tau_{\rm res}(0) \approx 2.5$ and $\tau_{\rm res}(1)/\tau_{\rm res}(0) \approx 5.4$ (Fig. 4). The robust content of this estimate is its *sign* (D_2O lengthens retention) and *order* (few-fold at partial substitution), not the precise value, which depends on $\Delta G_{\max}$ and on the measured g for PSD scaffolds.

A.4 Prediction 4 (isotopic titration of synaptic memory)

Prediction 4.

Raising the D_2O fraction of the bath lengthens AMPAR residence time and stabilizes LTP maintenance by a few-fold at partial substitution, with the magnitude tracking the measured cloud-point shift of the relevant PSD scaffolds; deuterium-depleted water produces the opposite, small effect. *Readout:* sptPALM/FRAP receptor retention and field-EPSP decay vs. graded D_2O. *Essential control:* D_2O is $\sim$25% more viscous than H_2O, which independently slows diffusion; the thermodynamic effect must be separated from this by a viscosity-matched H_2O+inert-crowder arm. *Falsified if* retention is unchanged after viscosity correction, or shifts with the opposite sign for a hydrophobically driven condensate.

A.5 A conjectural vibrational bridge

The thermodynamic prediction above stands on its own. We note—and explicitly label as conjecture—that isotopic substitution also shifts the vibrational spectrum of the hydrogen-bond network ($\omega \propto m^{-1/2}$, so H$\to$D lowers proton-dominated mode frequencies by up to $\sqrt{2}$), and that a prior proposal [16] speculates such collective modes participate in intracellular information processing. Whether the same isotopic perturbation that Eq. (13) predicts will change receptor retention *also* alters any functionally relevant condensate vibrational mode is untested, is not assumed anywhere in this paper, and is not needed for Prediction 4. We flag the possibility only to mark where the present, conservative model and that more radical proposal could in principle make contact—through a single, measurable control variable (solvent isotope) acting on a single, well-defined material (the PSD condensate)—and leave the vibrational question open.

A.6 Source Code

All source code to generate data and figures is at: https://github.com/brentharts/PSDmodel

References

[1] Zeng M., et al. (2018). Reconstituted postsynaptic density as a molecular platform for understanding synapse formation and plasticity. *Cell* 174(5), 1172–1187. https://doi.org/10.1016/j.cell.2018.06.047

[2] Chen X., Wu X., Wu H., Zhang M. (2020). Phase separation at the synapse. *Nat. Neurosci.* 23, 301–310. https://doi.org/10.1038/s41593-019-0579-9

[3] Site-specific phosphorylation of PSD-95 dynamically regulates the postsynaptic density as observed by phase separation (2021). *bioRxiv* 2021.03.03.433754. https://doi.org/10.1016/j.isci.2021.103268

[4] Takeshi Kaizuka, et al. (2024) FAM81A regulates condensation of postsynaptic proteins via liquid–liquid phase separation. [PSD LLPS meta-analysis / FAM81A.] https://doi.org/10.1371/journal.pbio.3002006

[5] Chen X., Cai Q., Zhou J., Pleasure S.J., Schulman H., Zhang M., Nicoll R.A. (2024). CaMKII autophosphorylation is the only enzymatic event required for synaptic memory. *PNAS* 121(26), e2402783121. https://doi.org/10.1073/pnas.2402783121

[6] Karl Ulrich Bayer and Karl Peter Giese (2024) A revised view of the role of CaMKII in learning and memory. *Nat. Neurosci.* https://doi.org/10.1038/s41593-024-01809-x

[7] Bowen Jia, et al. (2025) Shank3 oligomerization governs material properties of the postsynaptic density condensate and synaptic plasticity (2025). *Cell*. https://doi.org/10.1016/j.cell.2025.07.047

[8] Xi Liu, Yu Wang, et al. (2026) Dynamic recruitment of CaMKII into SHANK3 phase-separated condensates tunes postsynaptic density remodeling during long-term potentiation. *Nat. Commun.* https://doi.org/10.1038/s41467-026-72234-w

[9] Choi J.-M., Holehouse A.S., Pappu R.V. (2020). Physical principles underlying the complex biology of intracellular phase transitions. *Annu. Rev. Biophys.* 49, 107–133. https://doi.org/10.1146/annurev-biophys-121219-081629

[10] Nair D., et al. (2013). Super-resolution imaging reveals that AMPA receptors inside synapses are dynamically organized in nanodomains. *J. Neurosci.* 33(32), 13204–13224. https://doi.org/10.1523/jneurosci.2381-12.2013

[11] MacGillavry H.D., Song Y., Raghavachari S., Blanpied T.A. (2013). Nanoscale scaffolding domains within the postsynaptic density concentrate synaptic AMPA receptors. *Neuron* 78(4), 615–622. https://doi.org/10.1016/j.neuron.2013.03.009

[12] Nicoll R.A., Schulman H. (2023). Synaptic memory and CaMKII. *Physiol. Rev.* 103(4), 2897–2945. https://doi.org/10.1152/physrev.00034.2022

[13] Bielskutė S., Garcia-Cabau C., Frigolé-Vivas M., Szulc E., De Mol E., Pesarrodona M., García J., Salvatella X. (2021). Low amounts of heavy water increase the phase separation propensity of a fragment of the androgen receptor activation domain. *Protein Sci.* 30, 1427–1437. https://doi.org/10.1002/pro.4110

[14] Tempra C., Chamorro V.C., Jungwirth P. (2023). Effects of water deuteration on thermodynamic and structural properties of proteins and biomembranes. *J. Phys. Chem. B* 127, 1138–1143. https://doi.org/10.1021/acs.jpcb.2c08270

[15] Wang, Y., Zhu, L., Yang, Y. et al. (2026) Cellular water-potential sensing through biomolecular condensation. Nature 655, 1320–1329 https://doi.org/10.1038/s41586-026-10591-8

[16] Hartshorn B.S. (2026). Phonon-Mediated Biological Information Processing: The Cytoskeleton as an Acoustic Metamaterial for Non-Neural Agency. *Preprints* 2026, 2026040175. https://doi.org/10.20944/preprints202604.0175.v1

[17] Stephan Brown (2025) Quantum Biology of Cognition: A Unified Model for How Living Systems Turn Randomness into Meaningful Time https://ai.vixra.org/pdf/2512.0015v1.pdf